CANCER GENOMICS & PROTEOMICS *21*: 405-413 (2024)
doi:10.21873/cgp.20459

CEACAM6 Promotes Lung Metastasis *via* Enhancing Proliferation, Migration and Suppressing Apoptosis of Prostate Cancer Cells

ALIREZA SARAJI[1], KATHARINA WULF[1], JANINE STEGMANN-FREHSE[1], DUAN KANG[1], ANNE OFFERMANN[2], GEVORG SHAGHOYAN[1], DANNY JONIGK[3], MARK PHILIPP KÜHNEL[3], SVEN PERNER[4], JUTTA KIRFEL[1] and VERENA SAILER[1]

[1]*Pathology of the University Hospital Schleswig-Holstein, Lübeck, Germany;*
[2]*Institute of Pathology, University of Münster, Münster, Germany;*
[3]*Institute of Pathology, Uniklinik RWTH, Aachen, Germany;*
[4]*MVZ Center for Oncology, Tübingen, Germany*

Abstract. *Background/Aim: Metastatic prostate cancer (mPCa) results in high morbidity and mortality. Visceral metastases in particular are associated with a shortened survival. Our aim was to unravel the molecular mechanisms that underly pulmonary spread in mPCa. Materials and Methods: We performed a comprehensive transcriptomic analysis of PCa lung metastases, followed by functional validation of candidate genes. Digital gene expression analysis utilizing the NanoString technology was performed on mRNA extracted from formalin-fixed, paraffin-embedded (FFPE) tissue from PCa lung metastases. The gene expression data from primary PCa and PCa lung metastases were compared, and several publicly available bioinformatic analysis tools were used to annotate and validate the data. Results: In PCa lung metastases, 234 genes were considerably up-regulated, and 78 genes were significantly down-regulated when compared to primary PCa. Carcinoembryonic antigen-related cell adhesion molecule 6 (CEACAM6) was identified as suitable candidate gene for further functional validation. CEACAM6 as a cell adhesion molecule has been implicated in promoting metastatic disease in several solid tumors, such as colorectal or gastric cancer. We showed that siRNA knockdown of CEACAM6 in PC-3 and LNCaP cells resulted in decreased cell viability and migration as well as enhanced apoptosis. Comprehensive transcriptomic analyses identified several genes of interest that might promote metastatic spread to the lung. Conclusion: Functional validation revealed that CEACAM6 might play an important role in fostering metastatic spread to the lung of PCa patients via enhancing proliferation, migration and suppressing apoptosis in PC-3 and LNCaP cells. CEACAM6 might pose an attractive therapeutic target to prevent metastatic disease.*

Correspondence to: Verena-Wilbeth Sailer, Ratzeburger Allee 160, 23562, Lübeck, Germany. Tel: +49 45150015833, e-mail: verena-wilbeth.sailer@uksh.de

Key Words: Prostate cancer, CEACAM6, CD66c, microenvironment, lung metastases, bone metastases, gene expression, transcriptome analysis.

The majority of patients with prostate cancer (PCa) can be cured of their condition. When it comes to metastatic spread, the lung is the second most prevalent location after bones (1). PCa lung metastasis causes significant morbidity and mortality, and patients experience coughing, shortness of breath, and pleural effusion, all of which have a negative impact on their quality of life (2). There is consequently an urgent need for more clinical investigations to study the mechanisms behind metastatic disease and develop effective treatment strategies for patients suffering from metastasis diseases. Metastatic spread is a complicated, multistep process that was first proposed as a seed and soil concept in 1889 by Dr. Paget (3); however, since that time, the concept has undergone significant expansion (3, 4).

Unraveling the processes of PCa progression and metastatic spread might lead to a better understanding and ultimately better treatment or even prevention of lung metastases. We recently performed a comprehensive transcriptomic analysis of PCa lung metastasis. Interestingly, carcinoembryonic antigen cell adhesion molecule 6 (CEACAM6) was one of the candidate genes shown to be

overexpressed in PCa lung metastases, with levels more than 8-fold higher in lung metastases than bone metastases, when primary PCa was used as the reference.

CEACAM6 or CD66c belongs to a large family of adhesion molecules, which in turn belong to the immunoglobulin supergene family. Structurally, they have an extracellular domain and are anchored to the cell membrane (5). In normal tissues CEACAM6 is expressed on the surface of epithelial and myeloid cells (6). CEACAMs family have several biological functions, including immune response, angiogenesis, and pathogen receptors (7). Recently, CEACAMs family members were implicated in different types of cancer progression and tumorigenesis (8). For instance, CEACAM6 expression was reported as an adverse factor of overall survival in colorectal cancer (9); subsequently other research revealed that the expression of CEACAM6 mRNA has a significant role in predicting the peritoneal recurrence of gastric cancer (10). Another study found that non-invasive atypical breast lesions with high CEACAM6 expression exhibit a greater risk of progressing to invasive breast cancer (11). Furthermore, it has been found that CEACAM6 exerts its tumorigenic properties by enhancing adhesion and invasion in tumor and cancer cells (12). Currently, CEACAM6 has reported as an attractive target for antibody-conjugated and monoclonal therapies in cancer treatment due to its surface structure (13). However, there is little evidence implicating CEACAM6 in PCa progression and metastases. In one comprehensive study, Blumenthal *et al*. reported the elevation of CEACAM6 expression in a variety of solid tumors, including primary PCa tumors, suggesting potential involvement in metastasis spread (14). Based on the characteristics of cancer cells, PCa development is related to decreased cell apoptosis and enhanced cell viability, proliferation, and migration, which appear to be key criteria for the assessment of PCa cell functions (15, 16). Given the potential importance of CEACAM6 in tumorigenesis and metastatic spread, we performed a comprehensive transcriptomic analysis of PCa lung metastases to identify *CEACAM6* as the gene of interest, followed by functional validation on PCa cells (PC-3 and LNCaP) to determine CEACAM6 roles for PCa lung metastatic spread. The initial part of our study on PC-3 cells has been published as a preprint (17).

Materials and Methods

Ethics. This study was approved by the Ethics Committee of the University of Luebeck (project code 18-053, date of approval: March 2nd, 2018, date of amendment: June 17th, 2020). All methods in this study were performed in accordance with the relevant guidelines and regulations approved by University of Luebeck and University Hospital Schleswig-Holstein (UKSH) Luebeck.

FFPE samples. Formalin-fixed and paraffin-embedded (FFPE) material from primary prostate cancer along with prostate cancer lung and bone metastases (29 cases each) were selected from the archives of the Institute of Pathology, University Hospital Schleswig-Holstein (UKSH) Luebeck and the Research Center Borstel, Germany. Diagnosis of prostate cancer lung metastases was confirmed by a board-certified pathologist. Both primary and metastatic tumor samples were available for each patient.

mRNA extraction from FFPE. Hematoxylin and eosin (H&E) stained slides were evaluated by a pathologist (VS, AO) for tumor cell content and subsequently annotated for macrodissection. mRNA extraction was performed according to the standard protocols as we have described previously in detail (18). Briefly, the paraffin blocks were sectioned into 8 μm cuts and each slide was compared with the annotated H&E slide. Marked cancer tissue was scraped off with a scalpel and transferred directly to lysis buffer into an RNAase-free tube. RNA was isolated using the automatic bead-based Maxwell RSC RNA FFPE Kit (AS1440, Promega Corporation, Madison, WI, USA) according to the manufacturer's instructions. The RNA was eluted in water and then measured with Qubit™ (Life Technologies GmbH, Darmstadt, Germany). The RNA samples were divided into 7 μl aliquots and stored at –80˚C. Extracts with RNA concentrations of at least 10 ng/μl and sufficient RNA integrity with at least 90% of the fragments longer than 100 nucleotides were considered as suitable for gene expression analysis.

Digital gene expression analysis. Digital gene expression analysis using the Nanostring platform was performed as previously described (19, 20). A commercially available gene panel (nCounter PanCancer Progression Panel) consisting of 770 genes implicated in cancer progression and metastasis was employed. This gene panel consists of 277 angiogenesis-, 254 extracellular matrix-, 269 epithelial-mesenchymal transition, and 173 metastasis-related genes. Data were analyzed using the nSolver advanced analysis software provided by Nanostring (NanoString Tech. Inc., Seattle, WA, USA) (21).

Cell culture. For this work, we used the human PC-3 and LNCaP cell lines which were purchased from ATCC (Manassas, VA, USA) and maintained according to the provider's instructions. After thawing, the PC-3 cells were incubated at 37˚C with 5% CO_2 in DMEM medium (Gibco, Thermo Fisher Scientific Inc., Darmstadt, Germany) and the LNCaP cells were incubated at 37˚C with 5% CO2 RPMI medium (Gibco, Thermo Fisher Scientific Inc.). Both mediums were supplemented with 10% FBS and 1% penicillin-streptomycin (Gibco, Thermo Fisher Scientific Inc.). After reaching confluency of roughly 80% (3-7 days of incubation), the cells were washed with PBS two times and then detached from the culture dishes with the help of Accutase® or trypsin (ICT Inc., San Diego, CA, USA). The trypsinization was stopped by adding the DMEM/RPMI medium supplemented with 10% FBS and 1% penicillin-streptomycin to the cells respectively. The accruing suspension was then centrifugated at 800-1000 U/min at RT temperature for 10 min, then the supernatant was aspirated, and the pellet was resuspended in the respective medium. To measure the final cell concentrations of both cell lines, Pierce™ BCA Protein Assay Kit (Pierce, Thermo Fisher Scientific Inc.) was used according to the manufacturer's user guide. The suspension was split into bigger culture bottles or cultured into 6 well plates with 300K to 500K cells per well, respectively. Mycoplasma test was performed for detection of possible contaminations.

siRNA transfection in PC-3 and LNCaP cells. *CEACAM6* silencing was performed in PC-3 and LNCaP cells using Silencer® Select siRNAs purchased from Ambion® (Ambion, Thermo Fisher Scientific Inc.) targeting *CEACAM6* mRNA and scrambled RNA (Ambion, Thermo Fisher Scientific Inc.) as a non-targeting negative control. Cells were seeded into 6-well plates (300K-500K cells/well) and transfected in 2 ml of antibiotic-free medium with the transfection complex including 100 nM siRNA diluted in 300 µl/well of Opti-MEM™ medium (Gibco, Thermo Fisher Scientific Inc.) along with 5-7 µl/well Lipofectamine® 2000 (Thermo Fisher Scientific Inc.). After 5-6 h the medium was replaced with fresh and normal medium respectively.

siRNA sequences were as following: *CEACAM6* siRNA1, (sense 5'-ACUAAGUUGUAGAAAUUAATT-3', antisense 5'-UUAAUU UCUACAACUUAGUCT-3'); *CEACAM6* siRNA2, (sense 5'-CCAC UGCCAAGCUCACUAUTT-3', antisense: 5'-AUAGUGAGCUUG GCAGUGGTT-3'); negative control, (sense 5'-UUCUCCGAACGU GUCACGUTT-3', and antisense 5'-ACGUGACACGUUCGGAGA ATT-3').

Protein isolation and western blot analysis. Cells were detached from the culture bottles with trypsin and centrifugated at 1,000 rpm for 10 min. The supernatant was aspirated, and the cells were resuspended in warm PBS and again centrifugated at the same conditions as before. For protein isolation, a stock solution of 98% RIPA-buffer (Thermo Fisher Scientific Inc.) 1% of each protease-inhibitor (Cat. No. 87785) and 1% of phosphatase-inhibitor (Cat. No. 78440) was used. The cells were washed with cold PBS and resuspended in RIPA lysis buffer. This mixture incubated for 30 min stored on ice and then was centrifugated at 14,000 rpm at 4˚C for 10 min. The supernatant was collected.

For the protein assay, the Pierce™ BCA Protein Assay Kit was utilized. For that purpose, 9 µl of RIPA-buffer were put in each well of a 96-well plate and 1 µl protein-extract was added to each well. The working solution was added, and the plate was incubated at 37˚C for 30 min. The protein concentration of the samples was calculated based on the absorbance of the TECAN Spark® (Tecan Trading AG, Männedorf, Switzerland).

For western blot analysis, 30 µg of total protein was used for each line. After separating the isolated protein in 10 to 12% SDS polyacrylamide gel, they were transferred to a polyvinylidene fluoride membrane of 0.45 µm. The reaction was blocked with TBS-T buffer containing 6% non-fat dry milk and incubated with anti-CEACAM6, dilution 1:1,000 CEACAM6 recombinant rabbit monoclonal antibody (Cat. No. MA5-37801, Thermo Fisher Scientific Inc.) overnight at 4˚C. The abundant antibody-mixture was then washed off the membranes using TBS-T buffer in 3 cycles of 10 min each. Subsequently, anti-mouse IgG dilution 1:5,000 (Goat-anti-mouse IgG HRP, Cat. No. 31430, Thermo Fisher Scientific Inc.) was added to the washed membranes as a secondary antibody and the membranes were left for another hour of incubation at room temperature. After incubation, the membranes were washed for 10 min 5 ties in a row. The ECL substrate was used for illustration of the specific immune-reactive signals. Afterwards, the membranes were stripped, and beta-actin was added at 1:50000 (Cat. No. MA5-15739, Thermo Fisher Scientific Inc.) to the membranes as a positive control. The membranes were treated as described above.

CCK-8 assay. Cells were seeded into a 96-well plate at a density of 10^3-10^4 cells/well within 100 µl DMEM medium and incubated at 37˚C and 5% CO_2 for 24 h. Afterwards 10 µl of the CCK8 working solution were added to the wells and incubated under the same conditions again for 6 h. Then, 10 µl of CCK-8 were added to each well and the plate was incubated for 3 h one more time. Before measurement, the content of the wells was carefully mixed to make sure the color is distributed equally all over the well. The absorbance of the mixture in each well was then measured at a wavelength of 450 nm using a microplate reader.

Cell apoptosis assay (Caspase-3 activity). For the cell apoptosis assay, the Caspase-3/CPP32 Colorimetric Assay Kit (BioVision, Abcam, Cambridge, UK) was used according to the manufacturer's protocol. For the assay, apoptosis was induced in the cells and pellets of about 1×10^6 cells were resuspended in the cell lysis buffer. This mixture was positioned on ice to incubate for 10 min. After incubation the mixture was centrifugated and the supernatant was isolated for further usage. The extract was mixed with cell lysis buffer, 2X Reaction Buffer and 4 mM DEVD-pNA substrate and then left for incubation for about 1-2 h at 37˚C. The absorbance of the mixture in each well was measured at 405 nm wavelength by the help of TECAN Spark®.

Cell migration (cell scratch assay). For the cell migration assay, we used the well-known classical method. Briefly, the cells were seeded into a 6-well plate at 1×10^5 cells per well (two to three replicates per group). When the cells were 70-80% confluent, the transfection was performed according to the above-mentioned siRNA methods and after 6 h, the medium was removed and replaced with serum and antibiotics-free medium. Following starvation for 24 h, the monolayer cells were scratched (at least 2-3 even scratches per well) using a 200 µl pipette tip and washed three times with PBS to remove the detached and dead cells. Images were taken 0 and 24 h post-transfection (every 24 h after transfection until 48 h as maximum duration) under a light microscope, to measure the post-wounding widths of the scratches. At the end, the ratio of cell migration was calculated as following:

Cell migration rate=(scratch width at 0h - scratch width at 24/12h)/scratch width at 0 h.

Bioinformatics and statistical analyses. Several bioinformatic tools were manually applied for data enrichment and annotation. In particular, PANTHER (pantherdb.org) for information about the biological process, KEGG PATHWAY database (genome.jp/keg) for information about the pathways, Metascape (metascape.org) for information about the molecular function and Cytoscape (https://cytoscape.org) to calculate the key sub-clusters in the entire PPI network and the seed genes in each sub-cluster. An independent sample *t*-test was used to compare differences in mRNA counts in prostate cancer lung metastases and primary prostate cancer. Differentially expressed genes (DEGs) with log2 fold change >0 are considered as the meaningful and significantly expressed DEGs. Default parameters were set for calculation when STRING and MCODE were used. R (version 3.6.3) was used for graphing and data presentation.

Two samples were compared by utilization of student's two-tailed *t*-test. Comparisons of three or more samples were performed by usage of the one-way ANOVA with Tukey *post hoc* test. As a cutoff for statistical significance a *p*-Value of 0.05 was used. Data are shown as the mean and standard deviation. NanoString nSolver® analysis software v4.0 was used for analyzing Nanostring data and

A

Gene name	Accession #	Fold Change (FC)
CEACAM6	NM_002483.4	13.33
CD36	NM_000072.3	9.75
SLPI	NM_003064.2	9.01
FIGF	NM_004469.2	8.02
SPP1	NM_000582.2	7.59
SERPINA1	NM_000295.4	7.51
C3	NM_000064.2	6.62
ITGB6	NM_000888.3	5.9
CXCL17	NM_198477.1	5.63
S100A14	NM_020672.1	5.45

B

Gene name	Accession #	Fold Change (FC)
ACTG2	NM_001615.3	-11.1
SPOCK3	NM_001204355.1	-10.41
ISL1	NM_002202.2	-7.74
CNN1	NM_001299.4	-5.14
MYH11	NM_001040113.1	-5.14
RORB	NM_006914.3	-4.53
SLC44A4	NM_032794.1	-3.76
SMOC1	NM_001034852.1	-3.44
SFRP1	NM_003012.3	-3.3
RAMP1	NM_005855.2	-3.19

C

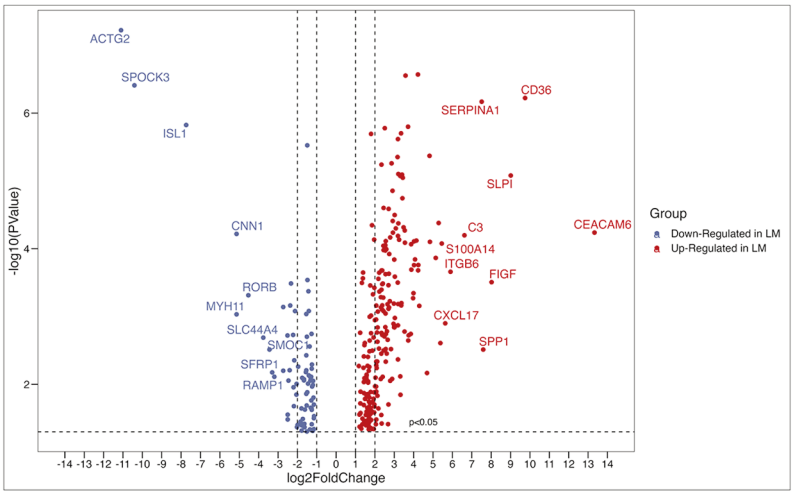

Figure 1. *Differentially expressed genes (DEGs) from transcriptome analysis of PCa lung metastasis. (A) Top 10 significantly up-regulated DEGs of PCa lung metastasis versus primary PCa based on fold change. (B) Top 10 significantly down-regulated DEGs of PCa lung metastasis versus primary PCa based on fold change. (C) Volcano plot representing the significant top 10 up- and down-regulated DEGs of PCa lung metastasis versus primary PCa based on fold change and p-Value; red dots represent up-regulated genes and blue dots represent down-regulated genes. n=24 FFPE samples of primary and metastatic PCa (24 out of 29 FFPE produced mRNA in sufficient quantity and quality).*

Prism® 6 (GraphPad Software Inc., San Diego, CA, USA) was used for statistical analyses. Sample sizes are mentioned in each figure.

Results

Transcriptomic expression of CEACAM6 in PCa lung metastasis. We performed a comprehensive transcriptome analysis of PCa lung metastases *versus* primary PCa tumors. Using NanoString nCounter technology, 24 of the 29 available FFPE produced mRNA in sufficient quantity and quality to effectively execute digital gene expression analysis (DGE). Setting primary PCa as a reference, we discovered that in PCa lung metastases 234 genes were significantly up-regulated, whereas 78 genes were considerably down-regulated (Supplementary Table I). Among these genes, we selected the top ten most significantly up-regulated and down-regulated differentially expressed genes (DEGs) (Figure 1A, B). Our bioinformatic analyses revealed that *CEACAM6*, based on fold change and *p*-value, had the highest score in PCa lung metastases *versus* primary PCa tumors (Figure 1C). The results for enrichment analyses are available in Supplementary Figure 1.

CEACAM6-targeting siRNAs efficiently suppress CEACAM6 expression in PC-3 and LNCaP cells. Given that PCa progression is associated with reduced cell apoptosis and increased cell viability, proliferation, and migration, we assessed the effect of CEACAM6 on these functions. For this purpose, we first established an efficient siRNA knockdown in PC-3 and LNCaP cells to assess the functional alteration caused by CEACAM6 knockdown in these cells.

To investigate the effect of *CEACAM6* silencing on PC-3 and LNCaP cells, the cells were transfected with different sequences of *CEACAM6*-siRNA. As a result, *CEACAM6*-siRNAs provided very high efficiency of gene expression knockdown in PC-3 and LNCaP cells (Figure 2A, B). Our siRNA experiment demonstrated more than 85% knockdown efficiency in PC-3 cells and 60% in LNCaP cells when compared to scrambled siRNA used as control (Figure 2C, D).

Knockdown of CEACAM6 elevated caspase-3 mediated apoptosis in PC-3 and LNCaP cells. It has previously been proposed that activation of caspase-3 is one of the key apoptotic mediators in PC-3 as well as LNCaP cells (22, 23). To determine the apoptotic properties in *CEACAM6* knockdown in these cells, we performed a caspase-3 assay 48 h after transfection by using a colorimetric caspase-3 activity kit. Our result demonstrated that caspase-3 activity was significantly increased in *CEACAM6* knockdown PC-3 and LNCaP cells compared to scrambled and WT cells (Figure 3A, B).

CEACAM6 knockdown inhibits the cell viability and proliferation in PC-3 and LNCaP cells. Transfected PC-3

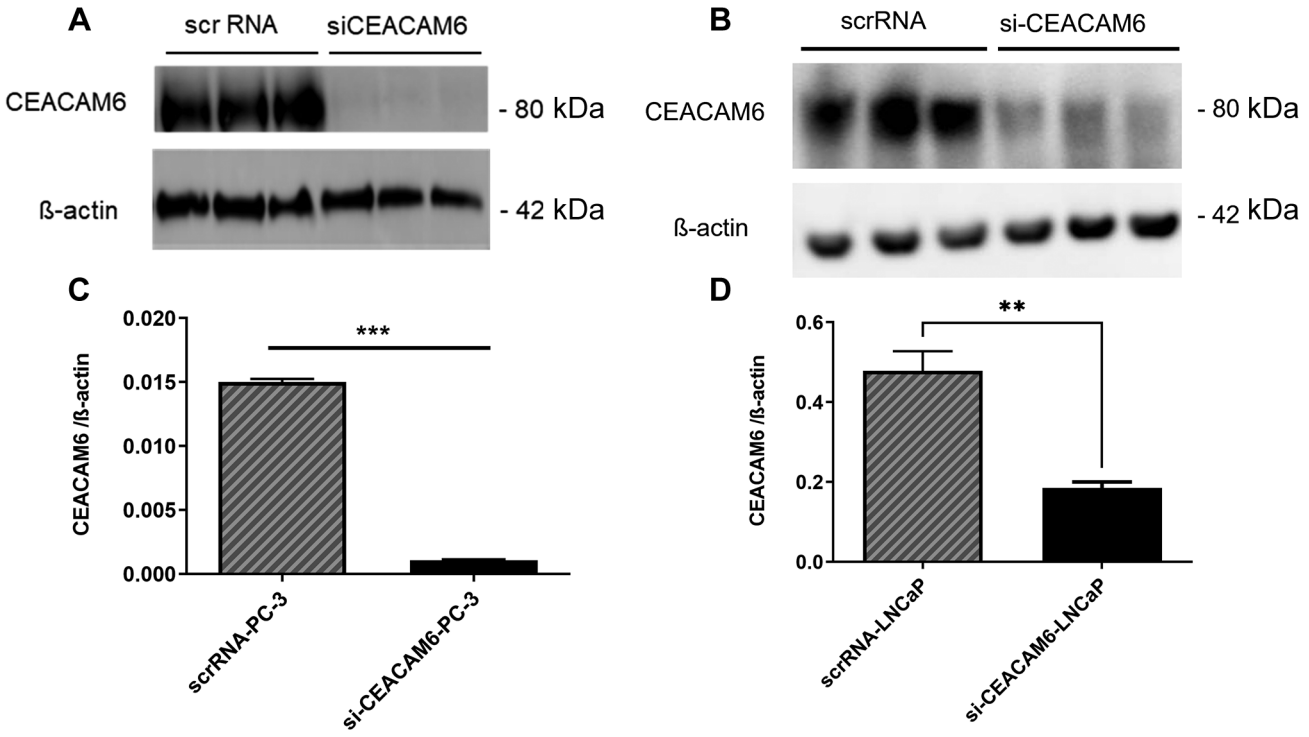

Figure 2. *CEACAM6-targeting siRNA effectively silences the expression of CEACAM6 in PC-3 and LNCaP cells. (A, B) Representative western blots of successful CEACAM6 knockdown in PC-3 and LNCaP cells. (C, D) Quantification of the efficacy of siCEACAM6 in human PC-3 and LNCaP cells. n=6 in each group. **p<0.01 and ***p<0.001 compared to the respective controls. Data were analyzed by Student's t-test and are shown as mean±standard error of the mean (SEM).*

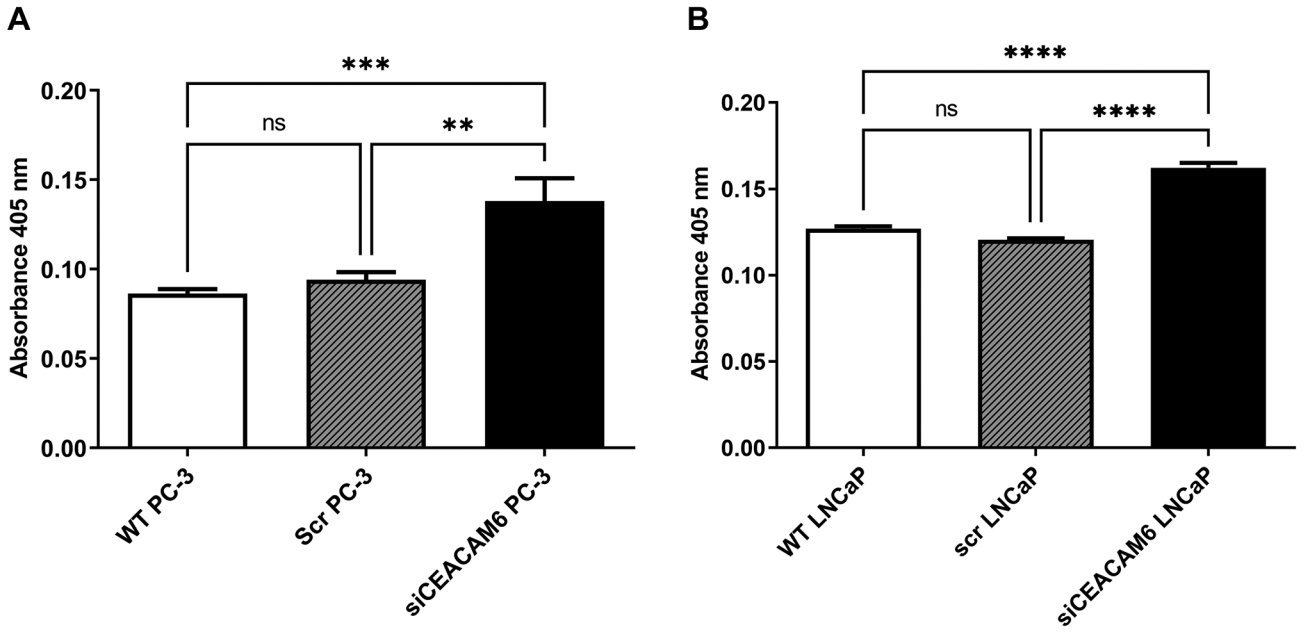

Figure 3. *Effects of CEACAM6 knockdown on the caspase-3 mediated apoptosis in PC-3 and LNCaP cells. Caspase-3 activity was detected by the caspase-3 assay kit. The absorbance at 405 nm was monitored 48 h after siRNA transfection in PC-3 (A) and LNCaP cells (B). n=7 in each group. **p<0.01, ***p<0.001 and ****p<0.0001 compared to the respective controls. Data were analyzed by one-way ANOVA with Tukey test and shown as mean±standard error of the mean (SEM).*

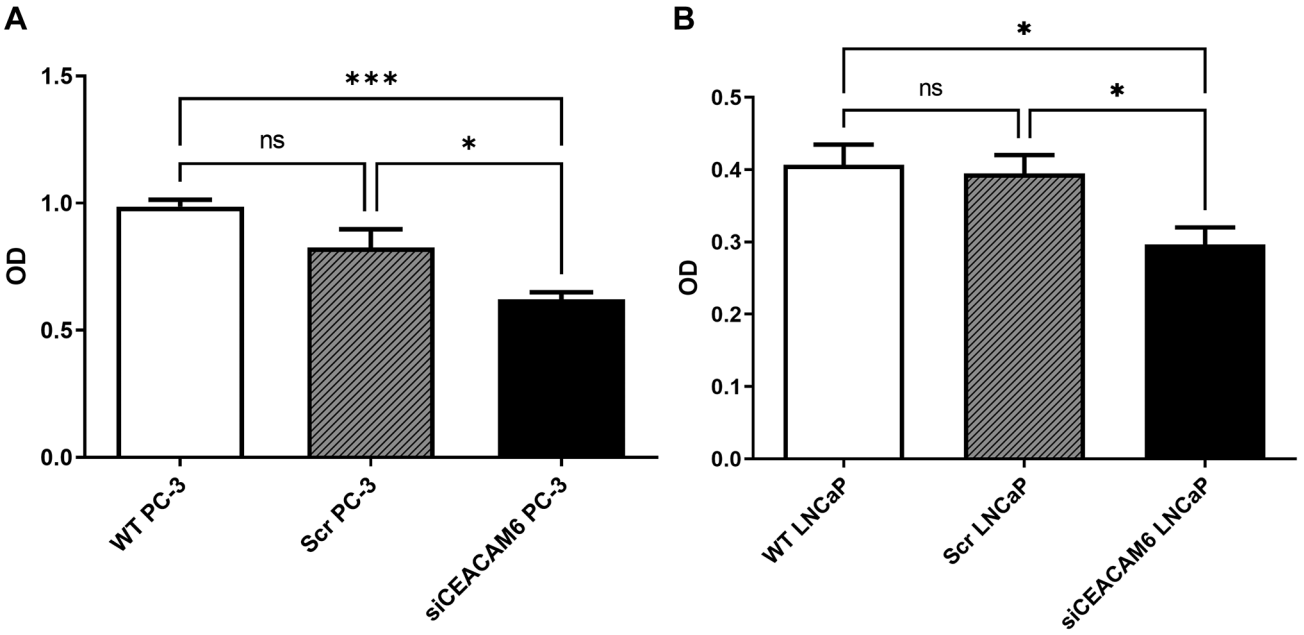

Figure 4. *Effects of CEACAM6 depletion on cell viability and proliferation of PC-3 and LNCaP cells. (A) PC-3 cell viability quantification by CCK-8 assay. The absorbance at 450 nm was monitored 48 h after siRNA transfection of PC-3 cells; n=10 in each group. (B) LNCaP cell viability quantification by CCK-8 assay. The absorbances at 450 nm was monitored 48 h after siRNA transfection of LNCaP cells; n=13 in each group. *p<0.05 and ***p<0.001 compared to the respective controls. Data were analyzed by one-way ANOVA with Tukey test and shown as mean±standard error of the mean (SEM).*

and LNCaP cells with *CEACAM6*-siRNA were assessed for the cell viability and proliferation assay by using the CCK-8 assay kit right after 48 h of transfection, using WT cells with no treatment and scrambled RNA (scrRNA) as controls. When compared to the controls, *CEACAM6* knockdown PC-3 and LNCaP cells showed a substantial reduction in cell viability and proliferation in both cell lines (Figure 4A, B).

CEACAM6 knockdown significantly diminished cell migration in PC-3 and LNCaP cells. Furthermore, we also investigated the effect of *CEACAM6* knockdown on the migration activities of PC-3 and LNCaP cells in terms of cell migration assay. To distinguish between the real migrant cells and proliferated cells, we minimized the basic proliferation ratio of the cells by using a serum-free growth medium during the scratch assay assessment. Our results showed that after 48 h of incubation post-transfection, the ratio of the migratory cells (PC-3 and LNCaP) with *CEACAM6* knockdown was significantly lower than that of the control groups (Figure 5A-D).

Discussion

We have performed a comprehensive gene expression analysis of PCa lung metastases using a digital comparative gene screening approach to unravel the unique transcriptional regulation of PCa pulmonary metastases. We identified a significant elevation of CEACAM6 in PCa lung metastases *versus* primary PCa. We next performed functional validation experiments using the classical siRNA to knockdown *CEACAM6* in PC-3 and LNCaP cell lines. We have selected PC-3 and LNCaP cell lines in our functional studies, because they are a well-known *in vitro* experimental model for advanced PCa (24). We were able to demonstrate that *CEACAM6* silencing altered functional hallmarks of PCa cells (PC-3 and LNCaP) including cell viability, proliferation, apoptosis, and cell migration, resulting in a less aggressive phenotype. Interestingly, our findings are consistent with some of previous investigations, where CEACAM6 was investigated in other type of cancer cells (12). Although the significance of CEACAM6 in PCa progression has yet to be thoroughly established, to the best of our knowledge, this is the first functional investigation that gives evidence that CEACAM6 does actually promote PCa aggressiveness to enable pulmonary spread. Meanwhile, in a very recent work by another group (25), CEACAM6 was reported as a significant up-regulated DEG in both lung and liver as visceral metastatic sites for PCa, which might offer additional relevance to our comparative analysis findings.

One criticism of the current study might be a lack of appropriate *in vivo* models. Unfortunately, *in vivo* models for metastatic diseases are extremely rare and difficult to obtain; so, in this investigation, we were unable to offer a complete *in*

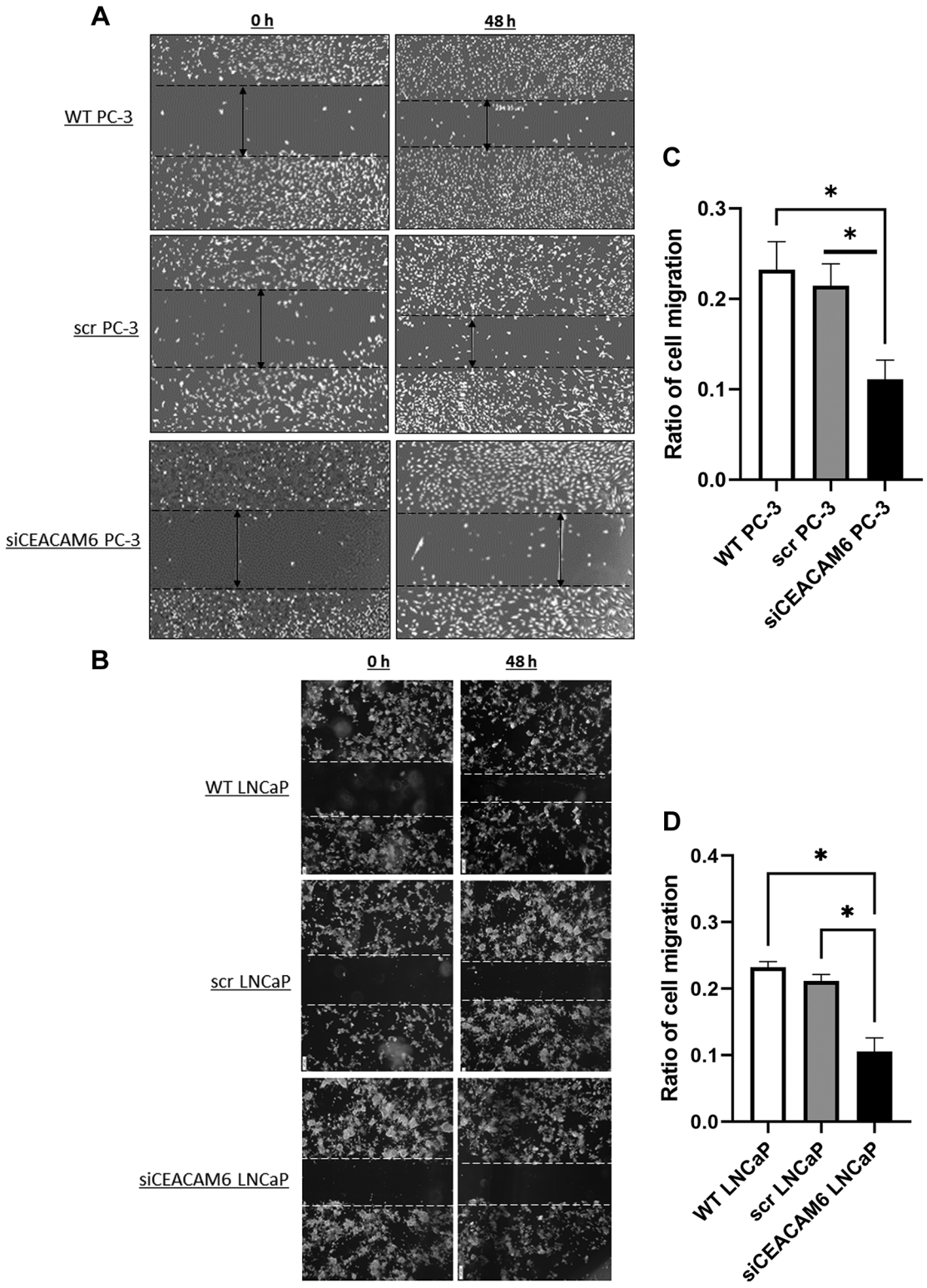

Figure 5. *The effects of CEACAM6 knockdown on PC-3 and LNCaP cell migration and motility. (A, B) Representative images of migration assay performed on PC-3 and LNCaP cells and monitored within 48 h post-transfection. Images were taken at indicated time points (time 0, 24 h and 48 h) and analyzed by the ImageJ software. (C, D) Quantification of the cell migration ratio of siCEACAM6, scrRNA and WT PC-3 and LNCaP cells; n=6 in each group. *p<0.05, compared to the respective control. Data were analyzed by one-way ANOVA with Tukey test and shown as mean±standard error of the mean (SEM).*

vivo model and instead relied solely on *in vitro* experiments. However, our results are promising enough to warrant further investigations. Despite the importance of the two PCa cell lines used here as a well-known model for studying the advanced stage of Pca (24, 26), additional available human Pca cell lines must be taken into consideration for future studies.

Recently, with regard to the importance of CEACAM family members in cancer and carcinogenesis, a fully-human anti-CEACAM5 antibody and chimeric antigen receptor T-cells have been developed for the treatment of CEACAM5-positive neuroendocrine Pca (27). CEACAM6 is also involved in suppressing T-cell mediated immune response and a CEACAM6-inhibitory antibody is now suggested to restore T-cell antitumor response in *in vitro* models of pancreatic, colorectal, and non-small cell lung cancers (28). In particular, because CEACAM6 is structurally a cell surface antigen, it should be further investigated as a potential solution for antibody-based treatment of cancer (7). As an example, Hagihara *et al*. suggested that neoadjuvant treatment with Sipuleucel-T in localized Pca induces gene expression of CEACAM6 and other immunoinhibitory genes. This suggests that combination treatment of Sipuleucel-T and anti-CEACAM6 antibodies could be a feasible option in advanced Pca treatment (29).

Conclusion

We conclude that *CEACAM6* promotes Pca aggressiveness and poses a very interesting therapeutic target in advanced Pca stages, particularly in terms of lung metastasis. However, additional investigation of the transcriptomic changes in the liver metastases and the role of CEACAM6 in its highly aggressive behavior must be taken into consideration. In addition, immunoinhibitory properties of *CEACAM6* as well as its tumor-promoting role should be further explored clinically.

Funding

This work was funded by Deutsche Forschungsgemeinschaft (DFG) Schwerpunktprogramm µBone SPP2084 (to vs. and SP).

Supplementary Material

Supplementary material is available at: https://doi.org/10.5281/zenodo.11109473

Conflicts of Interest

The Authors declare no potential conflicts of interest.

Authors' Contributions

VS, AS, AO, SP, JK, KW planned the study and methodology. AS, VS, DK, KW, DJ and MPK analyzed and interpreted the data. DK, AS and VS generated the bioinformatics data and methodology. JSF, KW, AO, VS, GS, AS performed experiments. VS and AS wrote the manuscript and prepared all figures. VS, AS, AO, SP, DK, JK, KW, DK, GS, DJ and MPK edited and reviewed the manuscript draft. All the above-mentioned Authors read and approved the final manuscript.

Acknowledgements

Duan Kang was supported by China Scholarship Council at the University of Luebeck (No. 202008440263). We thank Eva Dreyer for technical assistance.

References

1 Bubendorf L, Schopfer A, Wagner U, Sauter G, Moch H, Willi N, Gasser TC, Mihatsch MJ: Metastatic patterns of prostate cancer: An autopsy study of 1,589 patients. Hum Pathol 31(5): 578-583, 2000. DOI: 10.1053/hp.2000.6698

2 Teo MY, Rathkopf DE, Kantoff P: Treatment of advanced prostate cancer. Annu Rev Med 70: 479-499, 2019. DOI: 10.1146/annurev-med-051517-011947

3 Paget S: The distribution of secondary growths in cancer of the breast. 1889. Cancer Metastasis Rev 8(2): 98-101, 1989.

4 Liu Q, Zhang H, Jiang X, Qian C, Liu Z, Luo D: Factors involved in cancer metastasis: a better understanding to "seed and soil" hypothesis. Mol Cancer 16(1): 176, 2017. DOI: 10.1186/s12943-017-0742-4

5 Beauchemin N, Arabzadeh A: Carcinoembryonic antigen-related cell adhesion molecules (CEACAMs) in cancer progression and metastasis. Cancer Metastasis Rev 32(3-4): 643-671, 2013. DOI: 10.1007/s10555-013-9444-6

6 Schölzel S, Zimmermann W, Schwarzkopf G, Grunert F, Rogaczewski B, Thompson J: Carcinoembryonic antigen family members CEACAM6 and CEACAM7 are differentially expressed in normal tissues and oppositely deregulated in hyperplastic colorectal polyps and early adenomas. Am J Pathol 156(2): 595-605, 2000. DOI: 10.1016/S0002-9440(10)64764-5

7 Rizeq B, Zakaria Z, Ouhtit A: Towards understanding the mechanisms of actions of carcinoembryonic antigen-related cell adhesion molecule 6 in cancer progression. Cancer Sci 109(1): 33-42, 2018. DOI: 10.1111/cas.13437

8 Luebke AM, Ricken W, Kluth M, Hube-Magg C, Schroeder C, Büscheck F, Möller K, Dum D, Höflmayer D, Weidemann S, Fraune C, Hinsch A, Wittmer C, Schlomm T, Huland H, Heinzer H, Graefen M, Haese A, Minner S, Simon R, Sauter G, Wilczak W, Meiners J: Loss of the adhesion molecule CEACAM1 is associated with early biochemical recurrence in *TMPRSS2:ERG* fusion-positive prostate cancers. Int J Cancer 147(2): 575-583, 2020. DOI: 10.1002/ijc.32957

9 Jantscheff P, Terracciano L, Lowy A, Glatz-Krieger K, Grunert F, Micheel B, Brümmer J, Laffer U, Metzger U, Herrmann R, Rochlitz C: Expression of CEACAM6 in resectable colorectal cancer: a factor of independent prognostic significance. J Clin Oncol 21(19): 3638-3646, 2003. DOI: 10.1200/JCO.2003.55.135

10 Kaku H, Aoyagi K, Sudo T, Tanaka Y, Minami T, Isobe T, Kizaki J, Umetani Y, Murakami N, Fujita F, Akagi Y: Significance of intraperitoneal-free *KRT20* and *CEACAM6* mRNA expression for peritoneal recurrence of gastric cancer. Anticancer Res 42(8): 4003-4010, 2022. DOI: 10.21873/anticanres.15896

11 Poola I, Shokrani B, Bhatnagar R, DeWitty RL, Yue Q, Bonney G: Expression of carcinoembryonic antigen cell adhesion molecule 6 oncoprotein in atypical ductal hyperplastic tissues is associated with the development of invasive breast cancer. Clin Cancer Res 12(15): 4773-4783, 2006. DOI: 10.1158/1078-0432.CCR-05-2286

12 Blumenthal RD, Hansen HJ, Goldenberg DM: Inhibition of adhesion, invasion, and metastasis by antibodies targeting CEACAM6 (NCA-90) and CEACAM5 (carcinoembryonic antigen). Cancer Res 65(19): 8809-8817, 2005. DOI: 10.1158/0008-5472.CAN-05-0420

13 Cheng TM, Chang WJ, Chu HY, De Luca R, Pedersen JZ, Incerpi S, Li ZL, Shih YJ, Lin HY, Wang K, Whang-Peng J: Nano-strategies targeting the integrin αvβ3 network for cancer therapy. Cells 10(7): 1684, 2021. DOI: 10.3390/cells10071684

14 Blumenthal RD, Leon E, Hansen HJ, Goldenberg DM: Expression patterns of CEACAM5 and CEACAM6 in primary and metastatic cancers. BMC Cancer 7: 2, 2007. DOI: 10.1186/1471-2407-7-2

15 Kang J, La Manna F, Bonollo F, Sampson N, Alberts IL, Mingels C, Afshar-Oromieh A, Thalmann GN, Karkampouna S: Tumor microenvironment mechanisms and bone metastatic disease progression of prostate cancer. Cancer Lett 530: 156-169, 2022. DOI: 10.1016/j.canlet.2022.01.015

16 Zhang W, Hu C, Wang X, Bai S, Cao S, Kobelski M, Lambert JR, Gu J, Zhan Y: Role of GDF15 in methylseleninic acid-mediated inhibition of cell proliferation and induction of apoptosis in prostate cancer cells. PLoS One 14(9): e0222812, 2019. DOI: 10.1371/journal.pone.0222812

17 Saraji A, Wulf K, Stegmann-frehse J, Kang D, Offermann A, Kirfel J, Perner S, Sailer VW: Carcinoembryonic antigen-related cell adhesion molecule 6 (CEACAM6) promotes metastatic spread to the lung in advanced prostate cancer. Preprints, 2023. DOI: 10.20944/preprints202306.2221.v1

18 Saraji A, Offermann A, Stegmann-Frehse J, Hempel K, Kang D, Krupar R, Watermann C, Jonigk D, Kühnel MP, Kirfel J, Perner S, Sailer V: Cracking it - successful mRNA extraction for digital gene expression analysis from decalcified, formalin-fixed and paraffin-embedded bone tissue. PLoS One 16(9): e0257416, 2021. DOI: 10.1371/journal.pone.0257416

19 Saraji A, Duan K, Watermann C, Hempel K, Roesch MC, Krupar R, Stegmann-Frehse J, Jonigk D, Kuehnel MP, Klapper W, Merseburger AS, Kirfel J, Perner S, Offermann A, Sailer V: The gene expression landscape of prostate cancer BM reveals close interaction with the bone microenvironment. Int J Mol Sci 23(21): 13029, 2022. DOI: 10.3390/ijms232113029

20 Offermann A, Kang D, Watermann C, Weingart A, Hupe MC, Saraji A, Stegmann-Frehse J, Kruper R, Schüle R, Pantel K, Taubert H, Duensing S, Culig Z, Aigner A, Klapper W, Jonigk D, Philipp Kühnel M, Merseburger AS, Kirfel J, Sailer V, Perner S: Analysis of tripartite motif (TRIM) family gene expression in prostate cancer bone metastases. Carcinogenesis 42(12): 1475-1484, 2021. DOI: 10.1093/carcin/bgab083

21 Kaufmann S, Dennis L, Mashadi-Hossein A, Danaher P, Bailey C, Beechem J: Multiplexed cancer progression analysis using the ncounter® pancancer progression panel, 2019. Available at: https://nanostring.com/wp-content/uploads/WP_MK1189_Multiplexed_Cancer_Progression_Analysis.pdf [Last accessed on May 10, 2024]

22 Duan WR, Garner DS, Williams SD, Funckes-Shippy CL, Spath IS, Blomme EA: Comparison of immunohistochemistry for activated caspase-3 and cleaved cytokeratin 18 with the TUNEL method for quantification of apoptosis in histological sections of PC-3 subcutaneous xenografts. J Pathol 199(2): 221-228, 2003. DOI: 10.1002/path.1289

23 Slee EA, Adrain C, Martin SJ: Executioner Caspase-3, -6, and -7 perform distinct, non-redundant roles during the demolition phase of apoptosis. J Biol Chem 276(10): 7320-7326, 2001. DOI: 10.1074/jbc.M008363200

24 Sailer V, von Amsberg G, Duensing S, Kirfel J, Lieb V, Metzger E, Offermann A, Pantel K, Schuele R, Taubert H, Wach S, Perner S, Werner S, Aigner A: Experimental *in vitro*, *ex vivo* and *in vivo* models in prostate cancer research. Nat Rev Urol 20(3): 158-178, 2023. DOI: 10.1038/s41585-022-00677-z

25 Zhang P, Chen T, Yang M: Comparative analysis of prognosis and gene expression in prostate cancer patients with site-specific visceral metastases. Urol Oncol 42(5): 160.e1-160.e10, 2024. DOI: 10.1016/j.urolonc.2024.01.032

26 Moya L, Walpole C, Rae F, Srinivasan S, Seim I, Lai J, Nicol D, Williams ED, Clements JA, Batra J: Characterisation of cell lines derived from prostate cancer patients with localised disease. Prostate Cancer Prostatic Dis 26(3): 614-624, 2023. DOI: 10.1038/s41391-023-00679-x

27 Baek DS, Kim YJ, Vergara S, Conard A, Adams C, Calero G, Ishima R, Mellors JW, Dimitrov DS: A highly-specific fully-human antibody and CAR-T cells targeting CD66e/CEACAM5 are cytotoxic for CD66e-expressing cancer cells *in vitro* and *in vivo*. Cancer Lett 525: 97-107, 2022. DOI: 10.1016/j.canlet.2021.10.041

28 Pinkert J, Boehm HH, Trautwein M, Doecke WD, Wessel F, Ge Y, Gutierrez EM, Carretero R, Freiberg C, Gritzan U, Luetke-Eversloh M, Golfier S, Von Ahsen O, Volpin V, Sorrentino A, Rathinasamy A, Xydia M, Lohmayer R, Sax J, Nur-Menevse A, Hussein A, Stamova S, Beckmann G, Glueck JM, Schoenfeld D, Weiske J, Zopf D, Offringa R, Kreft B, Beckhove P, Willuda J: T cell-mediated elimination of cancer cells by blocking CEACAM6-CEACAM1 interaction. Oncoimmunology 11(1): 2008110, 2021. DOI: 10.1080/2162402X.2021.2008110

29 Hagihara K, Chan S, Zhang L, Oh DY, Wei XX, Simko J, Fong L: Neoadjuvant sipuleucel-T induces both Th1 activation and immune regulation in localized prostate cancer. Oncoimmunology 8(1): e1486953, 2018. DOI: 10.1080/2162402X.2018.1486953

Received April 3, 2024
Revised May 7, 2024
Accepted May 13, 2024